

# Accepted Manuscript

Application of broadband acoustic resonance dissolution spectroscopy (BARDS) to the gas release behaviour during rehydration of milk protein isolate agglomerates

Shaozong Wu, John Fitzpatrick, Kevin Cronin, M. Rizwan Ahmed, Dara Fitzpatrick, Song Miao



PII: S0260-8774(19)30056-1

DOI: <https://doi.org/10.1016/j.jfoodeng.2019.02.010>

Reference: JFOE 9526

To appear in: *Journal of Food Engineering*

Received Date: 21 November 2018

Revised Date: 8 February 2019

Accepted Date: 11 February 2019

Please cite this article as: Wu, S., Fitzpatrick, J., Cronin, K., Ahmed, M.R., Fitzpatrick, D., Miao, S., Application of broadband acoustic resonance dissolution spectroscopy (BARDS) to the gas release behaviour during rehydration of milk protein isolate agglomerates, *Journal of Food Engineering* (2019), doi: <https://doi.org/10.1016/j.jfoodeng.2019.02.010>.

This is a PDF file of an unedited manuscript that has been accepted for publication. As a service to our customers we are providing this early version of the manuscript. The manuscript will undergo copyediting, typesetting, and review of the resulting proof before it is published in its final form. Please note that during the production process errors may be discovered which could affect the content, and all legal disclaimers that apply to the journal pertain.

1 **Application of broadband acoustic resonance dissolution**  
2 **spectroscopy (BARDS) to the gas release behaviour during**  
3 **rehydration of milk protein isolate agglomerates**

4 **Shaozong Wu<sup>a,b</sup>, John Fitzpatrick<sup>b</sup>, Kevin Cronin<sup>b</sup>, M.Rizwan**  
5 **Ahmed<sup>c</sup>, Dara Fitzpatrick<sup>c</sup>, Song Miao<sup>a,\*</sup>**

6 <sup>a</sup> Teagasc Food Research Centre, Moorepark, Fermoy, Co. Cork, Ireland

7 <sup>b</sup> Process & Chemical Engineering, School of Engineering, University College Cork, Cork, Ireland

8 <sup>c</sup> Department of Chemistry, Analytical and Biological Chemistry Research Facility (ABCRF), University  
9 College Cork, Cork, Ireland\* Correspondence: song.miao@teagasc.ie; Tel.: +353-(0)-25-42468

10 **Abstract**

11 The BARDS technique was applied in this study to acoustically assess the  
12 rehydration behaviour of milk protein isolate (MPI) agglomerates and to compare  
13 with regular MPI powder. The results showed that BARDS has potential to monitor  
14 the rehydration behaviour of agglomerates. The greater porosity (> 70%) of  
15 agglomerated powders introduced more compressible gas into the water. The  
16 BARDS profile showed that there was faster initial gas release from the  
17 agglomerates, indicating better wetting and dispersion ability of the agglomerates  
18 with shorter  $t_M$  (time of maximum gas volume in solution). At 0.10% powder addition,  
19 agglomerated MPI reached  $t_M$  within 109 s, which was significantly less than the  
20 control MPI at 140 s. MPI with lactose binder (MPI-L) had a  $t_M$  of 80 s at 0.10%  
21 powder addition and, larger size MPI-L had a  $t_M$  of 60 s. At 0.20% and 0.30% powder  
22 addition, more time was required to wet and disperse the powders.

23 **Key words:** BARDS, milk protein isolate powder, rehydration, agglomeration

## 24 **1. Introduction**

25 Fluid-bed agglomeration is a technique that binds primary particles together to  
26 form aggregates with larger particle size. It can be applied to improve the physical  
27 properties of powders such as flowability and rehydration ability (Chever et al., 2017),  
28 and is used widely in the food industry. MPI (milk protein isolate) powder is an  
29 important product produced by the dairy industry, and is used as a milk protein  
30 ingredient in many food products. A major problem with MPI powder is its  
31 rehydration ability (Fitzpatrick et al., 2016). It is both a poor wetting and slowly  
32 dissolving powder (Crowley et al., 2015; Ji et al., 2015; Wu et al., 2019). The high  
33 content of casein present in MPI powder is considered as the major reason for its  
34 slow dissolution (Mimouni et al., 2010). Crowley et al. (2015) characterised the  
35 rehydration ability of milk protein concentrate (MPC) powders with milk protein  
36 concentrations ranging from 35 to 90%. They showed that increasing protein content  
37 reduced powder wettability. It also reduced powder dissolution ability especially at  
38 protein contents of 70% and higher. Ji et al (2015) showed that fluid-bed  
39 agglomeration could greatly improve the wettability of MPI powder, as the larger  
40 agglomerate particle size made it easier for water to penetrate the interstitial spaces  
41 between the particles. However, it did not improve the speed of dissolution of the  
42 particles once they were wetted and dispersed. In fact, agglomeration caused the  
43 dissolution to be slightly slower because a short period of time was required to  
44 break-up the agglomerate structure into the primary particles, which then dissolved  
45 slowly like in the regular MPI powder.

46 The dissolution process of powder in principle includes the gas exchange between  
47 powder and solution, that is, the gas inside the powder particles is released into the  
48 water as water penetrates into the particles and dissolves the powder material.  
49 However, the literature mainly focuses on the dissolution of material in powder form  
50 (Felix da Silva et al., 2018). Furthermore, when powder is re-structured by  
51 agglomeration, the air distribution in the powder is inevitably altered. The air release  
52 behaviour of agglomerated powder during rehydration is rarely discussed even  
53 though this can potentially provide important insights into the rehydration process.

54 Broadband acoustic resonance dissolution spectroscopy (BARDS) is a technique  
55 that can monitor gas release from powder in solution. The gas release has response  
56 in the acoustic resonance, which is influenced by the changes in the medium due to  
57 the release of air bubbles into the solvent during powder dissolution. The frequency  
58 change of BARDS results from the alteration of the speed of sound in the solvent  
59 containing air bubbles. Hence, the real-time information in the solvent can be  
60 monitored acoustically by changes in frequency (Fitzpatrick et al., 2014). So  
61 theoretically, the rehydration process of a dissolving powder can be described  
62 acoustically by BARDS. The first application of BARDS to the rehydration of dairy  
63 powder was reported for MPC powders with protein contents ranging from 35 to 90%  
64 (Vos et al., 2016). Rehydration of the different MPCs was monitored using BARDS,  
65 from which their rehydration characteristics were acoustically distinguished. The  
66 higher protein content powders showed slower gas release, which is indicative of  
67 slower rehydration behaviour. (Peddapatla et al., 2017) applied BARDS to  
68 investigate the wettability of pharmaceutical blends. Very poor wetting blends did not  
69 disperse into water and thus there was no gas release, while good wetting blends

70 readily dispersed and dissolved, releasing air bubbles that altered the frequency  
71 response measured by BARDS.

72 The objective of this study is to apply the BARDS technique for investigating the  
73 gas release of fluid-bed agglomerated MPI powders during rehydration and to  
74 compare this behaviour with that of regular unagglomerated MPI powder.  
75 Agglomeration of MPI was achieved using both water and lactose solution as binders  
76 to investigate the influence of binder type. The agglomerated MPI was sieved into  
77 two size fractions to investigate the influence of agglomerate particle size.

78

## 79 **2. Materials and methods**

### 80 **2.1. Materials**

81 Milk protein isolate (MPI) powder was purchased from Kerry Ingredients (Country  
82 Kerry, Ireland). The solids composition of the MPI powder is 86% protein, 1.5 % fat,  
83 6% ash and <1 % carbohydrate. Crystalline lactose powder was supplied by Arla  
84 Food Ingredients (Viby J, Aarhus, Denmark).

### 85 **2.2. Powder preparation**

86 The agglomerated MPI was prepared in a top-spray fluidised bed granulator (VFC-  
87 Lab Micro flo-coater, Vector Corporation, Iowa, USA). The quantity of MPI produced  
88 in each trial was 100 g. The volume of binder solution was 50 mL, and this was  
89 transferred by a peristaltic pump at a flowrate of  $1.2 \text{ mL} \cdot \text{min}^{-1}$ . The powder was  
90 fluidised in the bottom of the chamber by air at  $50^\circ\text{C}$ , while the binder was sprayed  
91 through a nozzle with a 1 bar pressure drop. After agglomeration, the powder was  
92 dried for 15 minutes by the air at  $50^\circ\text{C}$ . MPI agglomerates were produced using two

93 binders, one being water (MPI-W) and the other being a 15%, w/v lactose solution  
94 (MPI-L). Both MPI agglomerates were sieved to produce two size fractions with  
95 particle sizes between 106 and 180  $\mu\text{m}$  and 180 and 300  $\mu\text{m}$ .

## 96 **2.3. Physical properties of powder**

### 97 **2.3.1. Particle size**

98 Malvern Morphologi G3 (Malvern Instruments Ltd, Worcestershire, UK) was used  
99 to characterize the particle size distribution. A 15  $\text{mm}^3$  volume of powder was  
100 dispersed by air as a single layer of powder on a glass plate in the dispersion unit.  
101 The Morphologi G3 measured the number size distribution from which the volume  
102 size distribution was evaluated, along with corresponding  $D_{10}$ ,  $D_{50}$ , and  $D_{90}$  values.  
103 The experiment was performed in duplicate for each size distribution.

### 104 **2.3.2. Density and gas volume**

105 The loose bulk density ( $\rho_B$ ) and tapped bulk density ( $\rho_T$ ) of the MPI powder and its  
106 agglomerates were measured using a measuring cylinder and a tapping machine (Ji  
107 et al., 2015). The powder was tapped 500 times by the tapping machine (Funke  
108 Gerber, Berlin, Germany). The apparent density ( $\rho_A$ ) was measured by a helium gas  
109 pycnometer (AccuPyc II 1340, Micromeritics Instrument Corporation, Georgia, USA).  
110 The measurements were done in triplicate. The solid density ( $\rho_S$ ) of MPI and MPI-W  
111 was 1.53  $\text{g/mL}$ , while the MPI-L was 1.54  $\text{g/mL}$ . These were evaluated using the  
112 composition of MPI and its agglomerates (Niro, 2006).

113 In the MPI powder and its agglomerates, there are a number of void spaces where  
114 air resides, as illustrated in Fig. 1. In the MPI powder, there are vacuoles within the  
115 powder particles and interstitial air between powder particles in the bulk. A fluid-bed

116 agglomerate particle consists of primary particles bound together, thus there is  
 117 additional vacuole space between the primary MPI particles within the agglomerate  
 118 particle.

119 The porosity of the MPI powder and its agglomerates is defined in equation (1).

$$120 \quad \mathcal{E} = (\rho_A - \rho_T) / \rho_A \times 100 \quad (1)$$

121 For the MPI powder, this represents the void fraction associated with interstitial voids  
 122 in the tapped powder and possibly some vacuole voids within the primary particles,  
 123 but this does depend on whether or not the pycnometer gas penetrates inside the  
 124 primary particles. For the MPI agglomerates, the porosity includes additional voidage  
 125 associated with the voids between primary particles within the agglomerate particles,  
 126 as these are easily penetrated by the pycnometer gas.

127 The following specific air volumes are defined using the density data. These are  
 128 the bulk interstitial air (BIA), tapped occluded air (TOA) and vacuole occluded air  
 129 (VOA) specific volumes. These are defined in equations (2) to (4), and they are  
 130 expressed in units of mL / 100 g of powder.

$$131 \quad BIA = \left( \frac{1}{\rho_B} - \frac{1}{\rho_T} \right) \quad (2)$$

$$132 \quad TOA = \left( \frac{1}{\rho_T} - \frac{1}{\rho_A} \right) \quad (3)$$

$$133 \quad VOA = \left( \frac{1}{\rho_A} - \frac{1}{\rho_S} \right) \quad (4)$$

134 Chever et al. (2017) and GEA Niro (Niro, 2006) use similar definitions to characterise  
 135 specific air volumes in powder and agglomerates.

#### 136 2.4. The measurement of BARDS

137 The BARDS apparatus consists of a rehydration vessel, which is a glass vessel  
138 with a magnetic stirring bar, and a microphone placed 5 cm above the top rim of the  
139 glass vessel. A known mass of powder is dropped onto the surface of the water in  
140 the glass vessel. The broadband acoustic excitation is obtained from the tapping  
141 behaviour of a magnetic bar on the inner glass wall. The microphone captures the  
142 acoustic resonance from the sound travelling through the liquid, typically in the  
143 frequency range of 0-20 kHz. The BARDS instrument was stabilized for 30 s to allow  
144 a steady-state frequency to be achieved before powder is added (Ahmed et al.,  
145 2018). Gas is released from the powder which alters the measured frequency as the  
146 powder wets and dissolves. The frequency decreases over time until it attains a  
147 minimum value ( $f_{min}$ ), after which the frequency gradually returns to its original  
148 steady state value.

149 The volume of distilled water in the measuring vessel of BARDS was 25 mL.  
150 Three masses of each powder were used, that is 0.025 g, 0.0375 g and 0.05 g,  
151 giving powder concentrations in water of 0.1%, 0.15% and 0.2% w/v, respectively.  
152 The duration of the BARDS measurement was recorded over an 800 s duration and  
153 each test was carried out in duplicate. The stirring rate was 500 rpm in ambient  
154 temperature. The small masses of powder readily wetted and dispersed. A typical  
155 frequency profile over time is presented in Fig. 2. As stated above, the essence of  
156 the BARDS measurement technique is that as a powder dissolves in a liquid, it  
157 releases its entrained air to the (already saturated) liquid in the form of micro-  
158 bubbles and this correspondingly affects the frequency of sound in the liquid. The  
159 relationship between the frequency response and the fractional volume occupied by



160 the air bubbles is presented in equation (5), and details of this equation are provided  
161 by Fitzpatrick et al. (2012) and Crawford (1982).

$$162 \quad freq = \frac{freq_w}{\sqrt{1 + 1.49 \times 10^4 \cdot f_a}} \quad (5)$$

163 where  $f_a$  is the fractional volume occupied by air bubbles. The  $freq_w$  and  $freq$  are  
164 the frequency response of pure water in steady-state and bubble-filled water after  
165 adding sample, respectively. The equation and its parameter values are valid for the  
166 conditions prevailing for our work. The volume of gas ( $V_g$ ) in the water in the BARDS  
167 glass vessel can be calculated from equation (6), where  $V_w$  is the volume of water for  
168 rehydrating powders in BARDS.

$$169 \quad V_g = f_a \cdot V_w \quad (6)$$

## 170 **2.5 Statistical analysis**

171 One-way analysis of variance (ANOVA) was performed by SPSS software (IBM  
172 SPSS Statistics version 24). Duncan test was run for comparing the significance of  
173 multiple groups. The significance was set as  $P < 0.05$ .

174

## 175 **3. Results and discussion**

### 176 **3.1. Powder particle size, densities and specific gas volumes**

177 Particle size values for the MPI powder and its agglomerates are presented in  
178 Table 1. As expected, the particle size of agglomerated powders is much larger than  
179 that of the non-agglomerated powder. The  $D[v, 0.5]$  value of the MPI powder is 49.8  
180  $\mu\text{m}$ . The  $D[v, 0.5]$  values of the smaller size agglomerate fractions are 119  $\mu\text{m}$  for

181 MPI-W1 and 117  $\mu\text{m}$  for MPI-L1. The  $D[v,0.5]$  values of the larger size  
182 agglomerate fractions are 207  $\mu\text{m}$  for MPI-W2 and 168  $\mu\text{m}$  for MPI-L2. Powder  
183 agglomerated by water is larger than the powder agglomerated by lactose, especially  
184 for the larger size fractions. Jinapong et al. (2008) also observed that smaller sized  
185 soymilk agglomerates were obtained by increasing the concentration of maltodextrin  
186 binder from 0 to 10 %. Similarly, Szulc and Lenart (2013) showed that larger sized  
187 agglomerates were achieved using distilled water as the binder.

188 The powder densities of the MPI powder and its agglomerates are presented in  
189 Table 2. The apparent densities of the MPI powder and its agglomerates are all fairly  
190 similar with the agglomerates having slightly greater apparent densities ranging from  
191 1082 to 1119 g/L, and the MPI having a value of 1073 g/L, which is in line with a  
192 study by (Szulc and Lenart, 2013). The similar apparent densities are to be expected  
193 as the fluid-bed agglomerates are composed of primary MPI particles, and the  
194 pycnometer gas will penetrate them to the same extent whether they are in the MPI  
195 powder or the MPI agglomerates. The solid bridges in the agglomerate are possibly  
196 the reason why the agglomerates have slightly greater apparent densities. Table 2  
197 shows that both the loose and tapped bulk densities of the agglomerates are smaller  
198 than the MPI powder. This is to be expected because of the additional voids that  
199 exist between the primary particles within the agglomerate particles themselves. In  
200 relation to the agglomerates, the different particle size fractions showed different  
201 tapped bulk densities, with the smaller size fractions having larger tapped bulk  
202 densities.

203 The porosity of the powders was calculated in equation (1), using the apparent  
204 density and tapped bulk density. The porosity of the MPI powder and its  
205 agglomerates are presented in Table 2. The porosity of the agglomerates is greater

206 than that of the MPI powder, due to their lower tapped bulk densities as highlighted  
207 above. Likewise, the porosity of the larger sized agglomerates was significantly  
208 greater than the smaller sized agglomerates, while the type of binder had little effect  
209 on porosity.

210 The BIA, TOA and VOA specific volumes (equations 2-4) are presented in Table 3  
211 for the MPI powder and its agglomerates. The VOA had similar specific volumes in  
212 accordance with the apparent densities. This suggests that the pycnometer gas  
213 easily penetrates the porous structure between the primary particles in the  
214 agglomerates. The open pores in agglomeration possibly favour the gas penetration  
215 as well (Al hassn et al., 2018). Consequently, the VOA represents some or all of the  
216 specific air volume within the primary MPI particles, depending on the ability of  
217 pycnometer gas to penetrate into these particles. The VOA of primary MPI particle is  
218 probably dependent on the powder shrinkage during spray-drying (Foerster et al.,  
219 2016a; Foerster et al., 2016b; Fu et al., 2013). The TOA specific volumes have the  
220 same trend as porosity, with the agglomerates having larger TOA values than the  
221 MPI powder and the larger agglomerates have larger values than the smaller  
222 agglomerates. The TOA values represent the specific air volume between particles  
223 in the tapped bulk plus the specific air volume within the structure of the  
224 agglomerates and possibly some air volume within the primary MPI particles  
225 (depending on the ability of pycnometer gas to penetrate into these particles). The  
226 BIA values represent the change in specific volume between the loose and tapped  
227 bulks.

### 228 **3.2 BARDS profiles for MPI and agglomerated MPI**

229 This section compares the behaviour of agglomerated and non-agglomerated MPI,  
230 by initially comparing the BARDS profile of the MPI powder with one of the  
231 agglomerates, i.e. MPI-W2, at 0.1% w/v concentration of powder in water. The effect  
232 of agglomerate particle size, binder type and powder concentration in water are  
233 considered in subsequent sections. The BARDS acoustic profiles for the MPI powder  
234 and MPI-W2 are presented in Fig. 3a. For both powders, the frequency initially  
235 decreases to a minimum value and then increases gradually back to the original  
236 steady-state frequency. The change in frequency during powder rehydration is due  
237 to the change of the volume of gas in the water. The gas volume in water was  
238 estimated from equations (5) and (6) using the BARDS frequency data. The gas  
239 volume profiles for MPI and its agglomerate are presented in Fig. 3b. This shows a  
240 greater volume of gas release for the MPI agglomerate, which is to be expected  
241 considering its porosity is greater than the MPI powder. During the test, gas is being  
242 generated as gas is transferred from the particles into the water, and gas is being  
243 eliminated as gas leaves the surface of the water at the top of the vessel. The up-  
244 slope (Fig. 3b) indicates that gas generation rate is greater than gas elimination rate,  
245 and vice-versa during the down-slope. The frequency minimum or gas volume  
246 maximum indicates where the two rates are equal.

247 The time ( $t_M$ ) at which the maximum gas volume (or minimum frequency) occurs is  
248 indicative of the rehydration ability of the powder, with shorter times being indicative  
249 of faster or better rehydration ability (Peddapatla et al., 2017). Fig. 3 shows that the  
250 agglomerated MPI powder had a shorter  $t_M$  than the MPI powder. Table 4 shows that  
251  $t_M$  for the agglomerated powder and MPI powder were 85 s and 140 s, respectively.  
252 After  $t_M$ , Fig. 3 shows that return trajectories towards steady-state became similar  
253 with similar return times of about 450 s.

254 Previous work in the research group, conducted by Ji et al. (2015), experimentally  
255 compared the rehydration behaviour of MPI and agglomerated MPI. The wetting and  
256 dissolution behaviour of MPI and MPI agglomerates were measured. The MPI  
257 agglomerates in this BARDS study were prepared using the same techniques as  
258 presented by Ji et al. (2015) and had similar sizes and used the same binders. Ji et  
259 al. (2015) showed that agglomeration improved the wetting ability of the powder  
260 because it was easier for water to penetrate into the spaces between the larger sized  
261 agglomerate powder. Consequently, the agglomerated powder particles wetted more  
262 quickly and the agglomerate structure broke down readily liberating the primary MPI  
263 particles. This concurs with the BARDS profiles whereby the quicker wetting leads to  
264 faster release of interstitial gas and the break-up of the agglomerate structure  
265 leading to the release of vacuole air between the primary particles within the  
266 agglomerate structure. This results in greater gas release and a shorter  $t_M$ , as  
267 illustrated in Fig. 3b. This figure also shows that the MPI and the MPI agglomerate  
268 have similar return trajectories to steady-state, with both attaining steady-state at  
269 about 450 s. This can be explained by the gradual dissolution of the primary MPI  
270 particles, which was experimentally shown by Ji et al. (2015). Once the  
271 agglomerates wet and disintegrate to release the primary MPI particles, which is  
272 rapid, the rehydration is rate-limited by the dissolution of the MPI primary particles.

### 273 **3.3 Effect of particle size and binder**

274 Table 4 shows that all the agglomerates have shorter  $t_M$  times than the MPI  
275 powder and this is consistent for all three concentrations, highlighting the better  
276 wetting behaviour of the agglomerates. This is in line with the effect of granulation on  
277 powder wetting (Schuck, 2009). Furthermore, the return to steady-state trajectories

278 of all the agglomerates and the MPI powders are similar, as illustrated in Figs. 4 and  
279 5, which is indicative of the gradual dissolution of the MPI primary particles.

280 For the MPI agglomerates themselves, Table 4 shows that the larger sized  
281 agglomerates had shorter  $t_M$  times. This is due to faster wetting of larger sized  
282 particles, as water will penetrate more rapidly into the interstitial void spaces  
283 between the agglomerates. The faster wetting is also potentially due to the higher  
284 porosities (Table 2) and higher tapped occluded specific air volumes (Table 3) of the  
285 larger agglomerates. This may give rise to a more open porous structure within the  
286 larger agglomerates allowing water to penetrate more easily into the void spaces  
287 within the agglomerates and allowing gas to escape more rapidly. This is consistent  
288 with another study showing that large particles forming large pores and high porosity  
289 favour fast wetting (Gaiani et al., 2005). Furthermore, the effect of agglomerate size  
290 is consistent for all three concentrations.

291 The effect of the binder (water vs lactose solution) is also presented in Table 4.  
292 Shorter  $t_M$  times were obtained for lactose agglomerates containing the lactose  
293 binder. This occurs consistently at all three concentrations. The agglomerates with  
294 lactose and water binders have very similar porosities (Table 2), thus it is not a  
295 porosity effect. It is most likely because the lactose containing bridges are more  
296 hydrophilic (Li et al., 2016), which more rapidly dissolve resulting in easier break-up  
297 of agglomerates and release of air into the water. The presence of lactose can inhibit  
298 protein interaction and pave the way for water transfer within micelles during the  
299 rehydration process (Baldwin, 2010).

300 The trends presented by BARDS above are in line with work presented by Ji. et al.  
301 (2016), which also showed that larger agglomerate particle size and lactose binder

302 resulted in faster wetting. This shows that the BARDS technique is effective at  
303 assessing these effects on the rehydration behaviour of the MPI agglomerates.

### 304 **3.4 Effect of concentration**

305 As expected, Fig. 5 shows that there is more gas volume released by powder at  
306 higher concentrations of powder in water, simply because there is more powder  
307 present. Table 4 shows that there is a general trend that increasing the concentration  
308 of powder in water from 0.1% to 0.15% to 0.2% results in an increase in the  $t_M$  times  
309 for the MPI and all the MPI agglomerates. For example increasing the concentration  
310 from 0.1% to 0.2% resulted in  $t_M$  increasing from 140 s to 244 s for the MPI powder,  
311 and from 60 s to 80 s for the MPI-L2 powder. This is indicative of slower wetting at  
312 higher concentrations for all the powders, and shows that BARDS is effectively  
313 monitoring the influence of concentration. Furthermore, the return to steady-state  
314 took longer with increased concentrations, as illustrated in Figs. 4 and 5, with return  
315 times being about 450 s for the MPI powders and greater than 800 s for the higher  
316 concentrations. This is consistent with work conducted by Vos et al. (2016).

317 There are a number of reasons that potentially explain the effect of concentration  
318 on slowing the rehydration behaviour. The more powder that is added the longer it  
319 will take for all of the powder to wet and disperse, which is in agreement with a  
320 previous study (Fitzpatrick et al., 2014). A notable shift of time taken for the acoustic  
321 profiles returning to steady state from  $t_M$  was observed with more powder added. It  
322 will also result in more gas in the water which will take longer to be eliminated from  
323 the water. The more powder present will lead to more powder in solution which  
324 lowers the mass transfer driver and thus slows the rehydration process. The more  
325 powder present will also tend to increase viscosity which will slow the mass transfer

326 of water and gas between the particles and water, and slows the elimination of gas  
327 from the water.

#### 328 **4. Conclusion**

329 BARDS is a promising technique for studying the rehydration behaviour of powders  
330 by measuring the gas release behaviour over time. In this work, it was shown that  
331 the BARDS technique could be applied for assessing the rehydration behaviour of  
332 MPI agglomerates. Their faster gas generation showed that the agglomerates wetted  
333 and dispersed more rapidly than the regular MPI powder. The similar return  
334 trajectories to steady-state showed and the dissolution behaviours of the  
335 agglomerates were similar to that of the MPI and were rate-limited by the slow  
336 dissolution of the MPI primary particles. The technique was able to distinguish the  
337 different wetting and rehydration behaviours of different size agglomerates and  
338 agglomerates formed with different binders, because these factors influence the rate  
339 at which the agglomerates are wetted and rate at which the agglomerate structure  
340 disintegrates and releases gas. Overall, the study has shown that BARDS is a  
341 convenient, easy to use technique that can be applied to study the rehydration  
342 behaviour of agglomerates and to compare with the non-agglomerated powder.

#### 343 **Acknowledgement**

344 The authors would like to thank the financial support from China Scholarship Council  
345 (No.201606350091) and Teagasc project (0153).

#### 346 **Reference**

347 Ahmed, M.R., McSweeney, S., Kruse, J., Vos, B., Fitzpatrick, D., (2018). Contactless, probeless and  
348 non-titrimetric determination of acid-base reactions using broadband acoustic resonance dissolution  
349 spectroscopy (BARDS). *Analyst* 143(4), 956-962.



- 350 Al hassn, A.Z., Jeßberger, S., Hounslow, M.J., Salman, A.D., (2018). Multi-stage granulation: An  
351 approach to enhance final granule attributes. *Chemical Engineering Research and Design* 134, 26-35.
- 352 Baldwin, A.J., (2010). Insolubility of milk powder products – A minireview. *Dairy Science &*  
353 *Technology* 90(2-3), 169-179.
- 354 Chever, S., Mejean, S., Dolivet, A., Mei, F., Den Boer, C.M., Le Barzic, G., Jeantet, R., Schuck, P.,  
355 (2017). Agglomeration during spray drying: Physical and rehydration properties of whole milk/sugar  
356 mixture powders. *Lwt-Food Science and Technology* 83, 33-41.
- 357 Crawford, F.S., (1982). The hot chocolate effect. *American Journal of Physics* 50(5), 7.
- 358 Crowley, S.V., Desautel, B., Gazi, I., Kelly, A.L., Huppertz, T., O'Mahony, J.A., (2015). Rehydration  
359 characteristics of milk protein concentrate powders. *Journal of Food Engineering* 149, 105-113.
- 360 Felix da Silva, D., Ahrné, L., Ipsen, R., Hougaard, A.B., (2018). Casein-Based Powders: Characteristics  
361 and Rehydration Properties. *Comprehensive Reviews in Food Science and Food Safety* 17(1), 240-  
362 254.
- 363 Fitzpatrick, D., Evans-Hurson, R., Fu, Y., Burke, T., Kruse, J., Vos, B., McSweeney, S.G., Casaubieilh, P.,  
364 Keating, J.J., (2014). Rapid profiling of enteric coated drug delivery spheres via broadband acoustic  
365 resonance dissolution spectroscopy (BARDS). *Analyst* 139(5), 1000-1006.
- 366 Fitzpatrick, D., Kruse, J., Vos, B., Foley, O., Gleeson, D., O'Gorman, E., O'Keefe, R., (2012). Principles  
367 and applications of broadband acoustic resonance dissolution spectroscopy (BARDS): a sound  
368 approach for the analysis of compounds. *Anal Chem* 84(5), 2202-2210.
- 369 Fitzpatrick, J.J., van Lauwe, A., Coursol, M., O'Brien, A., Fitzpatrick, K.L., Ji, J.J., Miao, S., (2016).  
370 Investigation of the rehydration behaviour of food powders by comparing the behaviour of twelve  
371 powders with different properties. *Powder Technology* 297, 340-348.
- 372 Foerster, M., Gengenbach, T., Woo, M.W., Selomulya, C., (2016a). The impact of atomization on the  
373 surface composition of spray-dried milk droplets. *Colloids Surf B Biointerfaces* 140, 460-471.
- 374 Foerster, M., Gengenbach, T., Woo, M.W., Selomulya, C., (2016b). The influence of the chemical  
375 surface composition on the drying process of milk droplets. *Advanced Powder Technology* 27(6),  
376 2324-2334.
- 377 Fu, N., Woo, M.W., Selomulya, C., Chen, X.D., (2013). Shrinkage behaviour of skim milk droplets  
378 during air drying. *Journal of Food Engineering* 116(1), 37-44.
- 379 Gaiani, C., Banon, S., Scher, J., Schuck, P., Hardy, J., (2005). Use of a turbidity sensor to characterize  
380 micellar casein powder rehydration: Influence of some technological effects. *Journal of Dairy Science*  
381 88(8), 2700-2706.
- 382 Ji, J.F., Cronin, K., Fitzpatrick, J., Fenelon, M., Miao, S., (2015). Effects of fluid bed agglomeration on  
383 the structure modification and reconstitution behaviour of milk protein isolate powders. *Journal of*  
384 *Food Engineering* 167, 175-182.
- 385 Jinapong, N., Suphantharika, M., Jamnong, P., (2008). Production of instant soymilk powders by  
386 ultrafiltration, spray drying and fluidized bed agglomeration. *Journal of Food Engineering* 84(2), 194-  
387 205.
- 388 Li, K., Woo, M.W., Selomulya, C., (2016). Effects of composition and relative humidity on the  
389 functional and storage properties of spray dried model milk emulsions. *Journal of Food Engineering*  
390 169, 196-204.
- 391 Mimouni, A., Deeth, H.C., Whittaker, A.K., Gidley, M.J., Bhandari, B.R., (2010). Investigation of the  
392 microstructure of milk protein concentrate powders during rehydration: alterations during storage. *J*  
393 *Dairy Sci* 93(2), 463-472.
- 394 Niro, G., (2006). A11a-Particle density, occluded air and interstitial air by air pycnometer. GEA  
395 Process Engineering A/S, Gladsaxevej, Denmark.
- 396 Peddapatla, R.V.G., Ahmed, M.R., Blackshields, C.A., Sousa-Gallagher, M.J., McSweeney, S., Kruse, J.,  
397 Crean, A.M., Fitzpatrick, D., (2017). Broadband Acoustic Resonance Dissolution Spectroscopy (BARDS)  
398 - A novel approach to investigate the wettability of pharmaceutical powder blends. *Mol Pharm.*  
399 Schuck, P., (2009). *Dairy-derived ingredients*. Woodhead Publishing Limited.

- 400 Szulc, K., Lenart, A., (2013). Surface modification of dairy powders: Effects of fluid-bed  
401 agglomeration and coating. *International Dairy Journal* 33(1), 55-61.
- 402 Vos, B., Crowley, S.V., O'Sullivan, J., Evans-Hurson, R., McSweeney, S., Krüse, J., Rizwan Ahmed, M.,  
403 Fitzpatrick, D., O'Mahony, J.A., (2016). New insights into the mechanism of rehydration of milk  
404 protein concentrate powders determined by Broadband Acoustic Resonance Dissolution  
405 Spectroscopy (BARDS). *Food Hydrocolloids* 61, 933-945.
- 406 Wu, S., Fitzpatrick, J., Cronin, K., Miao, S., (2019). The effect of pH on the wetting and dissolution of  
407 milk protein isolate powder. *Journal of Food Engineering* 240, 114-119.

**Table 1**

Particle size of MPI and MPI agglomerates.

Sample	MPI	MPI-W1	MPI-W2	MPI-L1	MPI-L2
D[V, 0.1] / $\mu\text{m}$	22.6 $\pm$ 1.4 <sup>a</sup>	47.7 $\pm$ 2.0 <sup>b</sup>	69.3 $\pm$ 9.3 <sup>c</sup>	53.0 $\pm$ 0.7 <sup>b</sup>	71.2 $\pm$ 2.2 <sup>c</sup>
D[V, 0.5] / $\mu\text{m}$	49.8 $\pm$ 2.5 <sup>a</sup>	118.8 $\pm$ 1.7 <sup>b</sup>	207.3 $\pm$ 15.5 <sup>d</sup>	117.3 $\pm$ 3.5 <sup>b</sup>	168.8 $\pm$ 9.3 <sup>c</sup>
D[V, 0.9] / $\mu\text{m}$	95.6 $\pm$ 2.1 <sup>a</sup>	193.0 $\pm$ 2.3 <sup>b</sup>	334.7 $\pm$ 20.0 <sup>d</sup>	189.8 $\pm$ 9.3 <sup>b</sup>	290.2 $\pm$ 14.6 <sup>c</sup>

**Table 2**

Densities and porosity of MPI and MPI agglomerates.

	MPI	MPI-W1	MPI-W2	MPI-L1	MPI-L2
Loose bulk density (g/L)	261 $\pm$ 2	226 $\pm$ 6	223 $\pm$ 18	218 $\pm$ 4	200 $\pm$ 6
Tapped bulk density (g/L)	431 $\pm$ 5	330 $\pm$ 6	277 $\pm$ 4	311 $\pm$ 0	265 $\pm$ 1
Apparent density (g/L)	1073 $\pm$ 83	1119 $\pm$ 22	1108 $\pm$ 39	1103 $\pm$ 5	1082 $\pm$ 31
Porosity %	59.5 $\pm$ 0.42	70.5 $\pm$ 0.49	75.0 $\pm$ 0.37	71.8 $\pm$ 0.04	75.5 $\pm$ 0.06

**Table 3**

Specific air volumes of MPI and MPI agglomerates: bulk interstitial air, tapped occluded air, vacuole occluded air.

	Unit	MPI	MPI-W1	MPI-W2	MPI-L1	MPI-L2
Bulk interstitial air	mL/ 100g	151 $\pm$ 0 <sup>b</sup>	140 $\pm$ 16 <sup>b</sup>	89 $\pm$ 22 <sup>a</sup>	139 $\pm$ 9 <sup>b</sup>	122 $\pm$ 16 <sup>ab</sup>
Tapped occluded air	mL/ 100g	139 $\pm$ 2 <sup>a</sup>	214 $\pm$ 5 <sup>b</sup>	271 $\pm$ 5 <sup>d</sup>	230 $\pm$ 0 <sup>c</sup>	284 $\pm$ 1 <sup>e</sup>
Vacuole occluded air	mL/ 100g	27.8 $\pm$ 1.0 <sup>c</sup>	24.0 $\pm$ 0.3 <sup>a</sup>	24.8 $\pm$ 0.4 <sup>ab</sup>	25.7 $\pm$ 0 <sup>b</sup>	27.5 $\pm$ 0.4 <sup>c</sup>

**Table 4**

Time ( $t_M$ ) at frequency minimum (or gas volume maximum) during BARDS test for MPI and MPI agglomerates.

Concentration (w/v)	Components	$t_M$ (s)
0.10 %	MPI	140
	MPI-W1	109
	MPI-W2	85
	MPI-L1	80
	MPI-L2	60
0.15 %	MPI	140
	MPI-W1	118
	MPI-W2	109
	MPI-L1	93
	MPI-L2	80
0.20 %	MPI	244
	MPI-W1	163
	MPI-W2	118
	MPI-L1	101
	MPI-L2	80

## FIGURES

### List of Figures

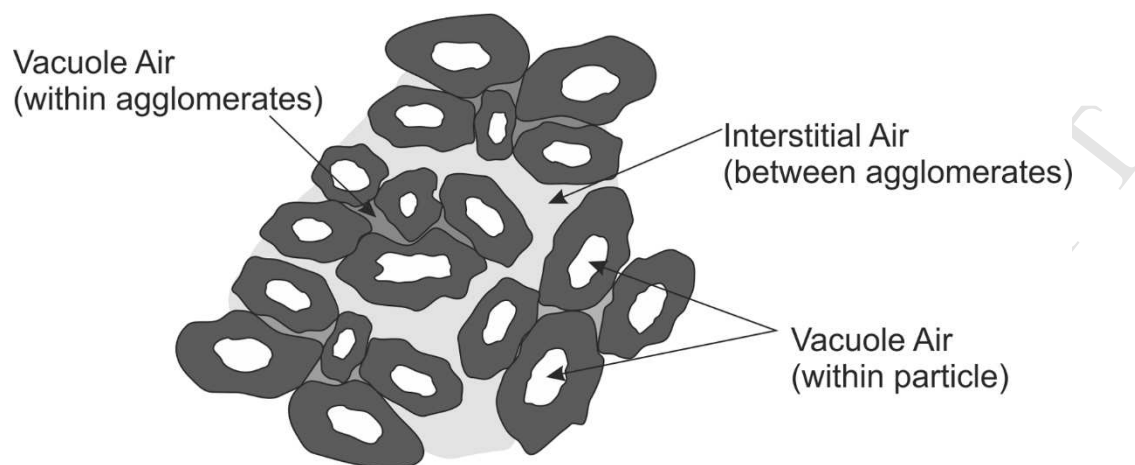
**Fig.1.** Illustration of air in agglomerated MPI powder: vacuole occluded air within primary MPI particles, occluded air between primary particles within agglomerates, and tapped interstitial air between agglomerates.

**Fig.2.** A representative spectrum of 0.025 g agglomerated MPI in BARDS, showing different phases of the spectrum.

**Fig.3.** (A) BARDS frequency spectrum and (B) gas volume profile of MPI and MPI-W2 agglomerate at 0.1 % concentration.

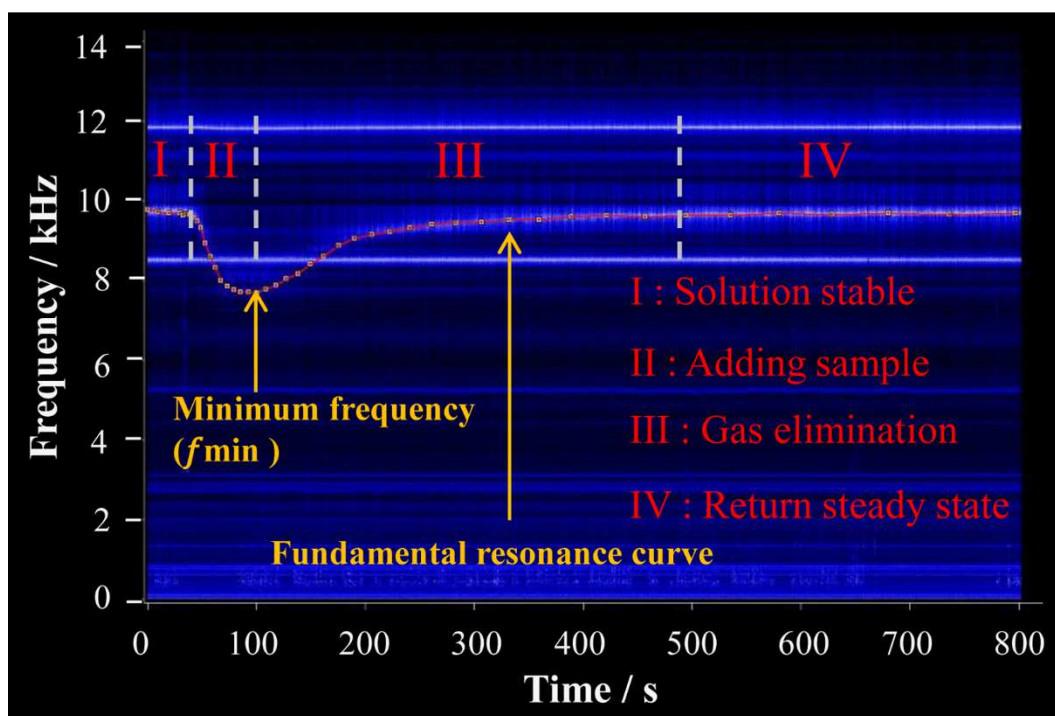
**Fig.4.** The BARDS frequency spectrum for MPI, MPI-W, MPI-L at concentrations of A: 0.1 %, B: 0.15 %, C: 0.2 %.

**Fig.5.** The gas volume profile for MPI, MPI-W, MPI-L at concentrations of A: 0.1 %, B: 0.15 %, C: 0.2 %.

**Fig.1**

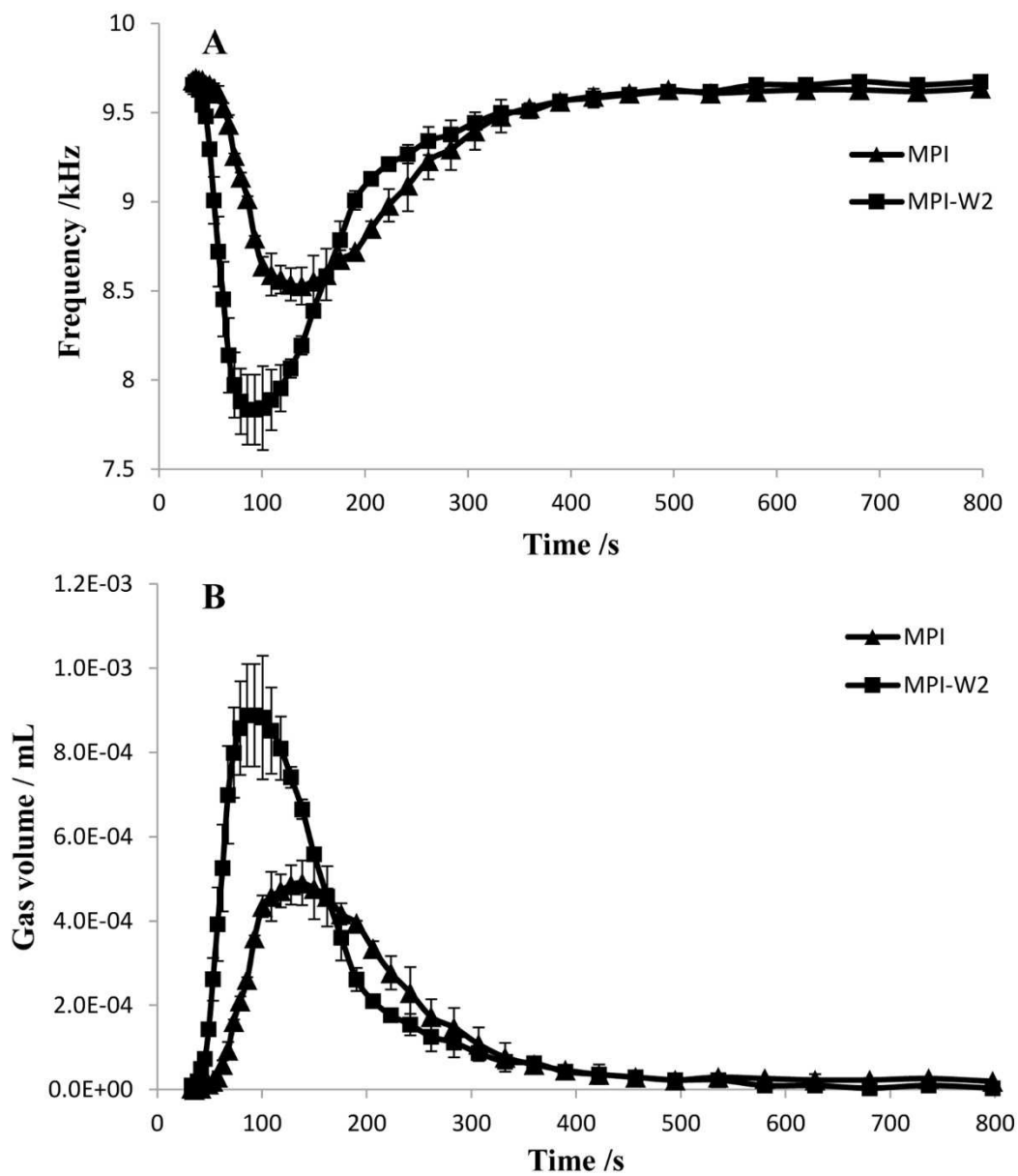
**Fig.1.** Illustration of air in agglomerated MPI powder: vacuole occluded air within primary MPI particles, occluded air between primary particles within agglomerates, and trapped interstitial air between agglomerates.

Fig.2



**Fig.2.** A representative spectrum of 0.025 g agglomerated MPI in BARDS, showing different phases of the spectrum.

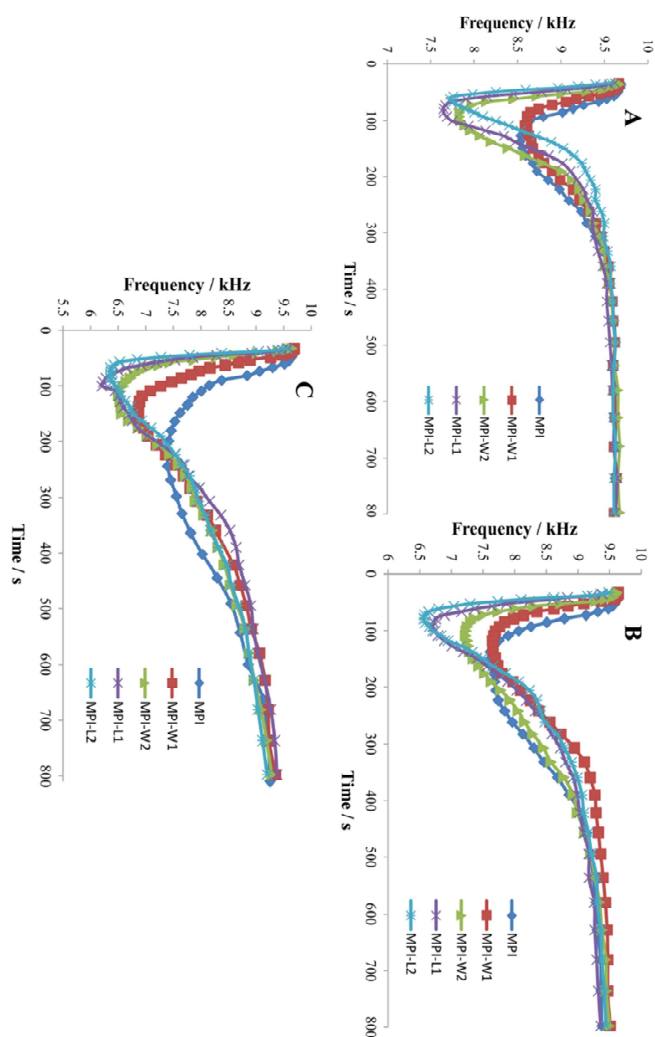
Fig.3



**Fig.3.** (A) BARDS frequency spectrum and (B) gas volume profile of MPI and MPI-W2 agglomerate at 0.1 % concentration.

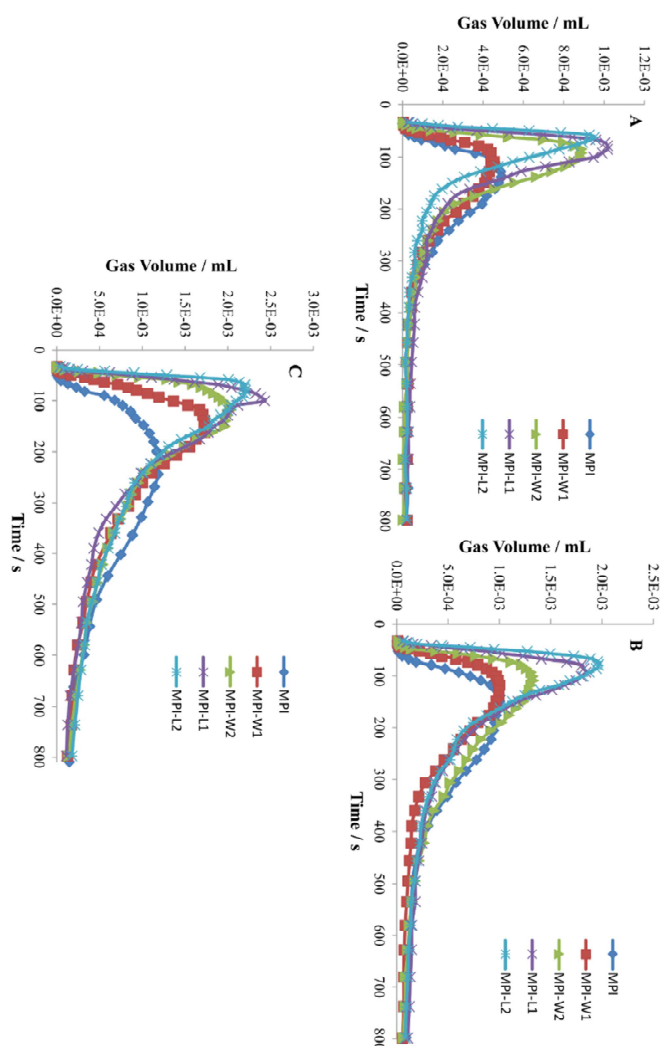


Fig.4



**Fig.4.** The BARDs frequency spectrum for MPI, MPI-W, MPI-L at concentrations of A: 0.1 %, B: 0.15 %, C: 0.2 %.

Fig.5



**Fig.5.** The gas volume profile for MPI, MPI-W, MPI-L at concentrations of A: 0.1 %, B: 0.15 %, C: 0.2 %.

## Highlights:

1. BARDS successfully monitored rehydration of MPI agglomerates.
2. BARDS showed that MPI agglomerates wetted more quickly than MPI powder.
3. BARDS showed that agglomerate size and binder type influenced rehydration.
4. Dissolution of MPI agglomerates was rate-limited by dissolution of primary MPI particles.